J Clin Monit Comput (2013) 27:147–155
DOI 10.1007/s10877-012-9403-8

ORIGINAL RESEARCH

Non-invasive accurate measurement of arterial PCO_2 in a pediatric animal model

Jorn Fierstra · Jeff D. Winter · Matthew Machina · Jelena Lukovic · James Duffin · Andrea Kassner · Joseph A. Fisher

Received: 25 April 2012 / Accepted: 12 October 2012 / Published online: 26 October 2012

Abstract The PCO_2 in arterial blood ($PaCO_2$) is a good parameter for monitoring ventilation and acid–base changes in ventilated patients, but its measurement is invasive and difficult to obtain in small children. Attempts have been made to use the partial pressure of CO_2 in end-tidal gas ($P_{ET}CO_2$), as a noninvasive surrogate for $PaCO_2$. Studies have revealed that, unfortunately, the differences between $P_{ET}CO_2$ and $PaCO_2$ are too variable to be clinically useful. We hypothesized that end-inspiratory rebreathing, previously shown to equalize $P_{ET}CO_2$ and $PaCO_2$ in spontaneously breathing humans, would also be effective with positive pressure ventilation. Eight newborn Yorkshire pigs were mechanically ventilated via a partial rebreathing circuit to implement end-inspiratory rebreathing. Arterial blood was sampled and tested for $PaCO_2$. A variety of alveolar ventilations resulting in different combinations of end-tidal PCO_2 (30–50 mmHg) and PO_2 (35–500 mmHg) were tested for differences between $P_{ET}CO_2$ and $PaCO_2$ (P_{ET}-aCO_2). The P_{ET}-aCO_2 of all samples was (mean ± 1.96 SD) 0.4 ± 2.7 mmHg. Our study demonstrates that, in ventilated juvenile animals, end-inspiratory rebreathing maintains P_{ET}-aCO_2 to what would be a clinically useful range. If verified clinically, this approach could open the way for non-invasive monitoring of arterial PCO_2 in critically ill patients.

Keywords Mechanical ventilation · Non-invasive · PCO_2 · Piglets · End-inspiratory rebreathing

J. Fierstra
Division of Neurosurgery, University Health Network, Toronto, ON, Canada
e-mail: jornfierstra@gmail.com

J. Fierstra
Rudolf Magnus Institute of Neuroscience, University Medical Center, Utrecht, The Netherlands

J. Fierstra
Division of Neuroradiology, Toronto Western Hospital, University Health Network, 3MC438, 399 Bathurst street, Toronto, ON M5T 2S8, Canada

J. D. Winter · J. Lukovic · A. Kassner
Department of Physiology and Experimental Medicine, The Hospital for Sick Children, Toronto, ON, Canada

J. D. Winter · J. Lukovic · A. Kassner
Department of Medical Imaging, The Hospital for Sick Children, 555 University Avenue, Toronto, ON M5G 1X8, Canada

M. Machina · J. Duffin · J. A. Fisher
Department of Physiology, Toronto General Hospital Research Institute, University of Toronto, Toronto, ON, Canada

M. Machina · J. Duffin · J. A. Fisher
Toronto General Hospital, University Health Network, 210 Dundas St. W. Suite 200, Toronto, ON M5G 2E8, Canada

J. Duffin · J. A. Fisher (✉)
Department of Anesthesiology, University Health Network, Toronto, ON, Canada
e-mail: joe.fisher@utoronto.ca

1 Introduction

During critical care, monitoring acid–base balance and the adequacy of ventilation, may require repeated invasive measurements of the partial pressure of CO_2 in arterial blood ($PaCO_2$) especially during weaning from mechanical ventilatory support. Repeated blood sampling places critically ill patients at risk for such associated complications as anemia [1], infection [2], arterial catheter blockage, and vascular endothelial injury and thrombosis. These risks are especially high in pediatric patients in whom the circulatory blood volumes, arteries and arterial catheters are smaller than in adults. In addition, drawing, transporting, and analyzing the samples consume considerable health care resources [1, 3].

By contrast, the partial pressure of CO_2 in end-tidal gas ($P_{ET}CO_2$) is a non-invasive, inexpensive measurement that ideally, would be used as a surrogate for $PaCO_2$ [2]. This relationship, however, cannot be relied on for all patients as other studies indicate that there are large and variable differences between $P_{ET}CO_2$ and $PaCO_2$ [2, 4]. Even after a measurement of a baseline partial pressure gradient of CO_2 between end-tidal gas and arterial blood (P_{ET}-aCO_2), the reliability of assuming changes in $PaCO_2$ from serial $P_{ET}CO_2$ measurements does not improve. Russel and Graybeal [5] and McDonald et al. [2] noted that in critically ill patients that suffered trauma, the changes in $PaCO_2$ were opposite to those of $P_{ET}CO_2$ in about 30 % of measures.

An alternative strategy has been to reduce the PCO_2 gradient between exhaled gas and the arterial blood. Ito et al. [6] administered exhaled gas at end inspiration in healthy seated spontaneously breathing volunteers and demonstrated that the P_{ET}-aCO_2 was reduced to within the range of error of measurement of $PaCO_2$. However, it is not known whether in the neonate, under the conditions of positive pressure ventilation and supine position, the effect of rebreathing at the end of inspiration on P_{ET}-aCO_2 would be maintained. To investigate this question, we used a ventilated pediatric animal model to determine the effect of end-inspiratory rebreathing on P_{ET}-aCO_2 and hypothesized that end-inspiratory rebreathing would reduce P_{ET}-aCO_2 at each combination of $P_{ET}CO_2$ and $P_{ET}O_2$.

2 Methods

The study was approved by our institutional animal care committee, and all procedures were conducted according to the guidelines of the Canadian Council on Animal Care. We studied 8 Yorkshire newborn pigs, 3–4 weeks of age with a mean weight of 3.6 kg (Table 1) in an animal operating room setting.

2.1 Animal preparation

Anesthesia was induced with a 0.2 ml/kg mixture of ketamine 58.8 mg/ml, acepromazine 1.18 mg/ml, and atropine 90 μg/ml administered by intramuscular injection, followed by 3 % isoflurane in O_2 to deepen anesthesia for surgical preparation. A catheter was inserted into the ear vein for continuous intravenous infusion anesthesia (22 mg/kg/h ketamine and 1 mg/kg/h midazolam). A 4 mm i.d. uncuffed pediatric endotracheal tube and a catheter for gas and pressure sampling were placed in the trachea via a tracheotomy. A catheter for arterial blood sampling was inserted into the carotid artery via surgical cut-down.

Piglets were initially mechanically ventilated via a pneumatic anesthesia ventilator (Air-Shields Ventimeter Controller IT, Air-Shields, Hatboro, PA 19040) with an O_2 and air mixture in pressure control mode with peak inspiratory pressures between 15 and 20 cmH_2O, PEEP 0 cmH_2O, frequency of 25–30/min, and inspiration:expiration ratio of 1:3 A sequential gas delivery circuit similar to that used for spontaneous ventilation [6, 7] was placed in a rigid container to form a functional “bag in box” secondary circuit (Fig. 1) and interposed between the ventilator and the endotracheal tube. This circuit was used both to change the end-tidal gas values as well as to apply end-inspiratory rebreathing. The circuit consists of a set of inspiratory and expiratory valves (i.e., a non-rebreathing valve), inspiratory and expiratory reservoirs (i.e., flexible bags) and a one way valve with slightly increased opening pressure connecting the expiratory reservoir to the inspiratory limb (‘cross-over valve’). During the expiratory phase, expired gas fills the expired reservoir and fresh gas fills the inspiratory reservoir, both displacing gas from the rigid container. This displaced gas is vented through the ventilator. On the inspiratory phase of the ventilator, the rigid box is pressurized. Fresh gas is progressively displaced from the inspiratory reservoir; once it is exhausted, the cross-over valve is forced open and the balance of the breath is supplied by previously exhaled gas being displaced from the expiratory gas reservoir. This results in the sequential delivery of the source gas (‘fresh gas’) followed by the rebreathed gas or its equivalent. Changes in alveolar ventilation are effected by controlling the concentrations of CO_2, O_2, and N_2 in a constant flow of inspired gas. In this way, the tidal volume, extent of rebreathing, and ventilatory frequency remains constant across the various alveolar gas concentrations. The gas input to the circuit (“fresh gas”) was provided by a computer-controlled gas blender (RespirAct^{TM}, Thornhill Research Inc., Toronto, Canada). The gas blender controls the flows of each source gas via a voltage controlled orifice (VSONC-6S11-VE-Q0, Parker, Cleveland, USA) and flow sensors (TSI Air 41221,

Table 1 Piglet baseline measurements, and necropsy findings

Piglet #	Weight (kg)	(ml/min)	PaO_2 (mmHg) (FiO_2 0.21)	PA-aO_2 (mmHg) (FiO_2 1.0)	Anatomical shunt[a]	Lung pathology[a]
1	3.1	75	87	137	PDA, PFO	Severe bilateral atelectasis
2	3.6	90	95	74	PDA, PFO	Severe bilateral atelectasis
3	3.8	100	65	301	PDA	Severe unilateral atelectasis
4	3.4	95	88	178	PDA	Bilateral atelectasis
5	3.5	90	71	418	PFO	Mild bilateral atelectasis
6	3.5	90	84	271	PDA	Severe unilateral atelectasis
7	3.8	95	81	304	PFO	None
8	4.2	90	75	430	None	None

PDA patent ductus arteriosus, *PFO* patent foramen ovale; $\dot{V}CO_2$, minute CO_2 production; PA-aO_2, alveolar (end-expired) to arterial O_2 partial pressure gradient, FiO_2 inspired fractional concentration of O_2

[a] Findings at necropsy

Shoreview MN, USA) using PID algorithms. A computer calculated the inspired concentrations of CO_2 and O_2 required to attain target $P_{ET}CO_2$ and $P_{ET}O_2$ using algorithms described by Slessarev et al. [7] An intra-tracheal catheter was used to monitor airway pressures and sample tidal gas. After the piglets were stabilized on the ventilator and secondary circuit, pancuronium bromide 0.2 mg/kg was administered intravenously as a bolus followed by an infusion at 0.1 mg/kg/h for the duration of the experiment. Tidal gas was sampled continuously and analyzed for PCO_2 (Ir3107, Servomex, Sugar Land, TX, USA) and PO_2 (UFO-130-2, Teledyne Analytical Instruments, City of Industry, CA, USA) from which $P_{ET}CO_2$ and $P_{ET}O_2$ were identified using specialized data acquisition software (LabView; National Instruments Corporation, Austin, TX). The real-time end-tidal picking algorithm was designed for spontaneously breathing, and ventilated subjects. The program time shifts the PCO_2 trace to synchronize with the airway pressure trace; it then finds the maximum PCO_2 value between the times of the two pressures that indicate peak inspiration. The data is then reviewed graphically and any errors in end-tidal picking are adjusted manually. All monitors measuring physiologic parameters were sampled at 20 Hz and recorded using the same data acquisition software.

2.2 Study protocol

PCO_2 and PO_2 tensions of the inspired gas were varied sequentially in the following three phases of the experiment (Fig. 2):

1. Isoxic ΔPCO_2: From the baseline condition ($P_{ET}CO_2$ = 40 mmHg, $P_{ET}O_2$ 100 mmHg), concentrations of CO_2 and O_2 in the inspired gas were sequentially altered to produce 10 mmHg isoxic step increases and decreases of $P_{ET}CO_2$ in random order, returning to baseline after each step change.
2. Isocapnic ΔPO_2. From the baseline condition, concentrations of CO_2 and O_2 in the inspired gas was sequentially altered to produce an isocapnic step

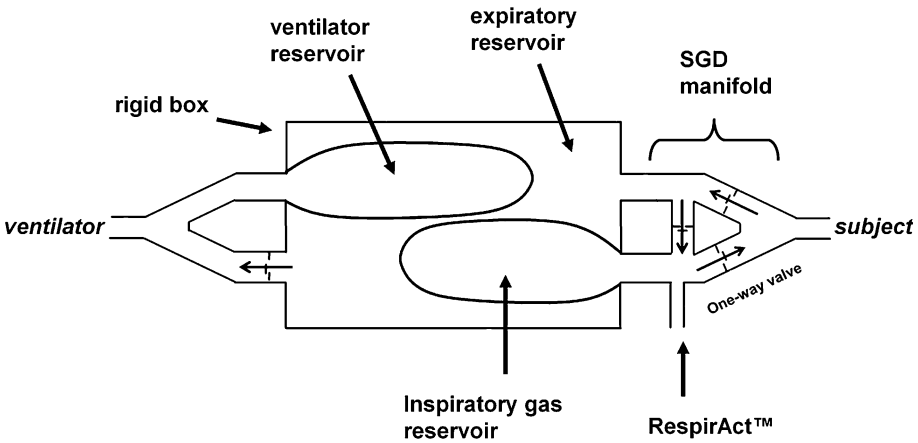

Fig. 1 The end-inspiratory rebreathing and inspiratory gas control circuit is interposed between the ventilator and the subject, with the circuit manifold part of the rigid box that acts as the expiratory gas reservoir and contains the inspiratory gas reservoir. During exhalation, gas from the RespirAct™ enters the inspiratory gas reservoir and exhaled gas enters the rigid container. During inspiration, the box is pressurized. The relative opening pressure of the one-way valves assures that the gas from the inspiratory gas reservoir is first displaced into the subject. Once the inspiratory gas reservoir empties, the valve in the cross-over limb opens and the ventilator displaces previously exhaled gas to the subject

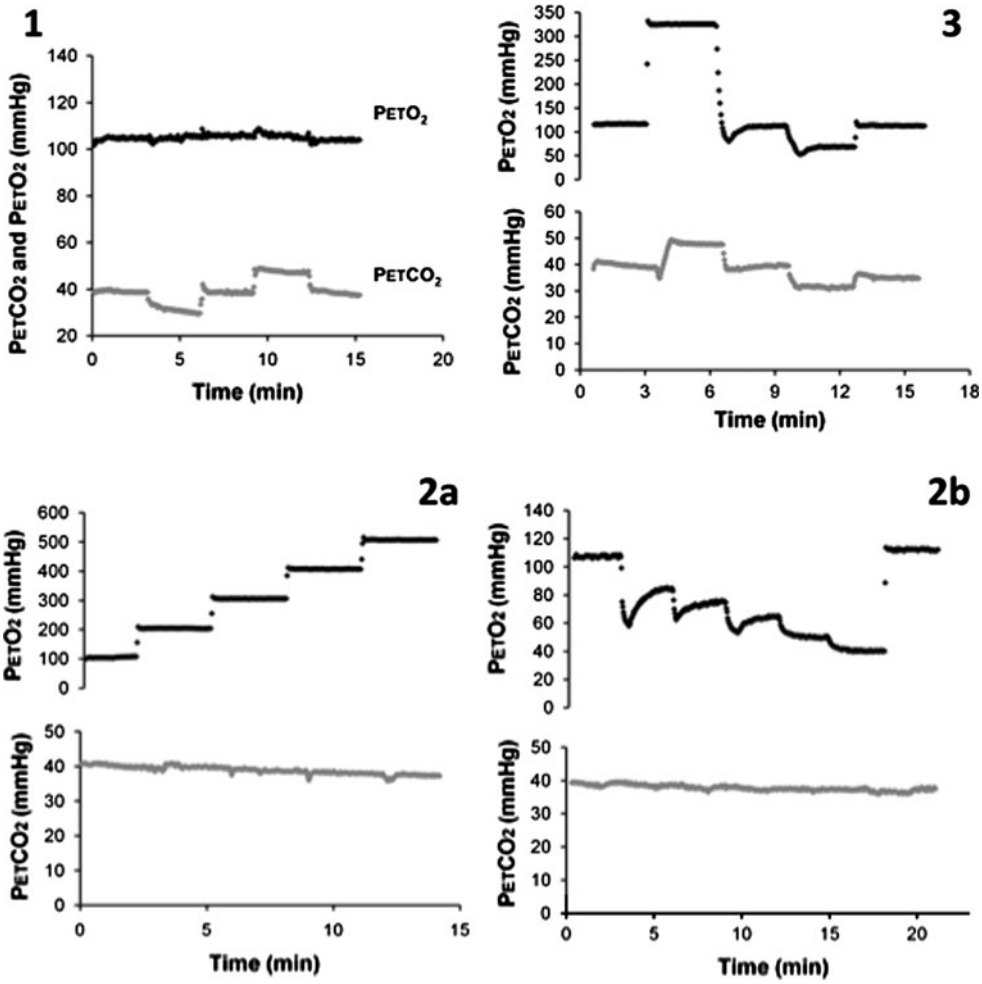

Fig. 2 Data for the test protocols from a representative piglet. Protocol *1* iso-oxic ΔPCO_2, *2a*, *2b* isocapnic ΔPO_2 *3* $\Delta PCO_2/\Delta PO_2$. Protocol 2 was divided into isocapnic hyperoxic step changes in $P_{ET}CO_2$ (*2a*) and isocapnic hypoxic step changes in $P_{ET}CO_2$ (*2b*). The protocol could not be carried out as a single protocol since the transition from hyperoxia (500 mmHg) back to baseline (100 mmHg) was not possible within the required 3 min mainly because of the small tidal volumes employed

increase in $P_{ET}O_2$ to 500 mmHg (protocol 2a) and a step decrease in $P_{ET}O_2$ to 35 mmHg (protocol 2b).

3. $\Delta PCO_2 + \Delta PO_2$. From baseline, concentrations of CO_2 and O_2 in the inspired gas were sequentially altered to produce periods of hypercapnia plus hyperoxia ($P_{ET}CO_2$ 50 mmHg + $P_{ET}O_2$ 300 mmHg), and hypocapnia plus hypoxia ($P_{ET}CO_2$ 30 mmHg + $P_{ET}O_2$ 60 mmHg) in a block fashion, returning to baseline between steps.

Each step change was maintained for 3 min, and $P_{ET}CO_2$ was taken as the average $P_{ET}CO_2$ of all breaths during the last minute of each step. An arterial blood sample was drawn during the last minute of each step, placed on ice, and analyzed within 30 min of collection (ABL 700, Radiometer Copenhagen, Denmark).

Ordinarily it may take many minutes—possibly hours—to develop a new steady state $P_{ET}CO_2$ and $PaCO_2$ after a change in ventilation. This is due to the time required for the inspiratory gas to come into equilibrium with the functional residual capacity and total body stores. These delays make it difficult to account for changes in non-measured variables over time in the results. We therefore developed our system to rapidly implement the equilibrium state. The computer prospectively calculates the inspired concentrations of CO_2 and O_2 required bringing the respective gas concentrations in the lungs and tissue gas stores to equilibrium at target levels [8]. After rapid equilibration with the lung, continued equilibration with the tissues ensues over the next few breaths by taking into account the ongoing gas equilibration with mixed venous blood in the lung and metabolic CO_2 production and O_2 consumption. Subsequent ventilation reflects a state of equilibrium (Fig. 2).

2.3 Statistics

Statistical analysis of the data was performed using the SAS System v.9.1.3 (SAS Institute Inc, Cary NC, USA). A series of mixed-effect repeated measures models was performed to determine whether differences in $P_{ET}CO_2$ and $PaCO_2$ values were significantly greater than zero, and whether the magnitude of these differences varied across

sequences, and across PCO_2 and PO_2 tensions. A subject identifier was included as a random effect in each of these models to account for the relatedness of observations taken on the same subject.

Two separate model analyses were conducted, the first to examine P_{ET}-aCO_2 as a function of sequence, and the second to examine P_{ET}-aCO_2 as a function of $P_{ET}CO_2$. Bonferroni-adjusted pairwise comparisons were used to examine whether P_{ET}-aCO_2 was significantly smaller in the sequence in which both $P_{ET}CO_2$ and $P_{ET}O_2$ were varied than in the sequence when $P_{ET}O_2$ was maintained constant. A Bland–Altman analysis (Bland and Altman) [9] was used to calculate the limits of agreement between $P_{ET}CO_2$ and $PaCO_2$. Data are presented as mean ± SD.

3 Results

3.1 Animal status

Although the animals assigned to this experiment seemed clinically healthy, necropsy revealed them to be otherwise. The study was performed in the autumn and many of the animals in the research facility had flu-like symptoms. At necropsy, most of the animals in our study had visible pulmonary infiltration in at least one of their lungs on gross examination (Table 1). A virology examination was not performed. Of the 8 animals in the study, 4 had a patent foramen ovale and 5 had a patent ductus arteriosus. Baseline PaO_2 tensions when breathing spontaneously (with some intermittent ventilatory assistance as required to prevent hypoventilation while titrating the level of anesthesia) on room air and on 100 % O_2 (indicating A-a O_2 gradients) are also presented in Table 1. In some piglets the A-a gradient was not commensurate with the degree of atelectasis. Piglets 1 and 2, in particular, had extensive atelectasis but normal A-a gradients. This probably reflected an increased vascular resistance and brisk hypoxic pulmonary vasoconstriction in the atelectatic areas. Data from a single representative piglet for each of the test protocols are presented in Fig. 2.

3.2 Controlling $P_{ET}CO_2$ and $PaCO_2$

Table 2 lists the differences between the target $P_{ET}CO_2$ (P_TCO_2) and measured $P_{ET}CO_2$ and $PaCO_2$ for all three protocols, and Fig. 3a, b illustrate these results. There was a small but consistent difference between P_TCO_2 and measured $P_{ET}CO_2$ ($p = 0.005$), which was marginally greater at a P_TCO_2 of 30 mmHg, compared to those at 40 and 50 mmHg ($p < 0.01$ for both).

3.3 P_{ET}-aCO_2

Table 3 lists the differences between measured $P_{ET}CO_2$ and $PaCO_2$ for all three protocols, and Fig. 4a and b illustrate these results. The average P_{ET}-aCO_2 difference was small but consistent ($p = 0.034$). Within each protocol, there were no significant differences between $P_{ET}CO_2$ and $PaCO_2$ but when the data across protocols were pooled,

Table 2 Differences between target end-tidal PCO_2 (P_TCO_2) and measured end-tidal PCO_2 (P_T-$_{ET}CO_2$) and measured arterial PCO_2 (P_T-aCO_2) values for each of the 3 protocols at each of the 3 targets in mmHg

Protocol	P_TCO_2	P_T-$_{ET}CO_2$		P_T-aCO_2	
		Mean ± SD	95 % CI	Mean ± SD	95 % CI
1	30	2.8 ± 3.0	(0.0, 5.6)	4.0 ± 2.9	(1.4, 6.7)
1	40	−0.8 ± 2.2	(−1.6, 0.1)	−1.3 ± 2.7	(−2.3, −0.3)
1	50	−1.0 ± 1.7	(−2.4, 0.5)	−1.4 ± 1.9	(−3.0, 0.1)
	Combined	−0.1 ± 2.6	(−0.9, 0.7)	−0.5 ± 3.2	(−1.5, 0.4)
2	30				
2	40	−1.5 ± 3.4	(−2.2, −0.8)	−1.9 ± 3.2	(−2.6, −1.2)
2	50				
	Combined	−1.5 ± 3.4	(−2.2, −0.8)	−1.9 ± 3.2	(−2.6, −1.2)
3	30	4.0 ± 4.9	(−0.5, 8.6)	4.7 ± 3.7	(1.3, 8.1)
3	40	−0.4 ± 3.2	(−1.9, 1.1)	−1.3 ± 2.8	(−2.5, −0.0)
3	50	−0.8 ± 2.9	(−3.5, 1.9)	−1.8 ± 4.1	(−5.6, 1.9)
	Combined	0.4 ± 3.9	(−0.9, 1.8)	−0.2 ± 4.0	(−1.6, 1.2)
Combined	30	3.4 ± 4.0	(1.2, 5.7)	4.4 ± 3.2	(2.5, 6.2)
Combined	40	−1.2 ± 3.2	(−1.7, −0.7)	−1.7 ± 3.0	(−2.2, −1.2)
Combined	50	−0.9 ± 2.3	(−2.1, 0.4)	−1.6 ± 3.0	(−3.3, 0.0)
	Combined	−0.7 ± 3.4	(−1.3, −0.2)	−1.2 ± 3.5	(−1.7, −0.7)

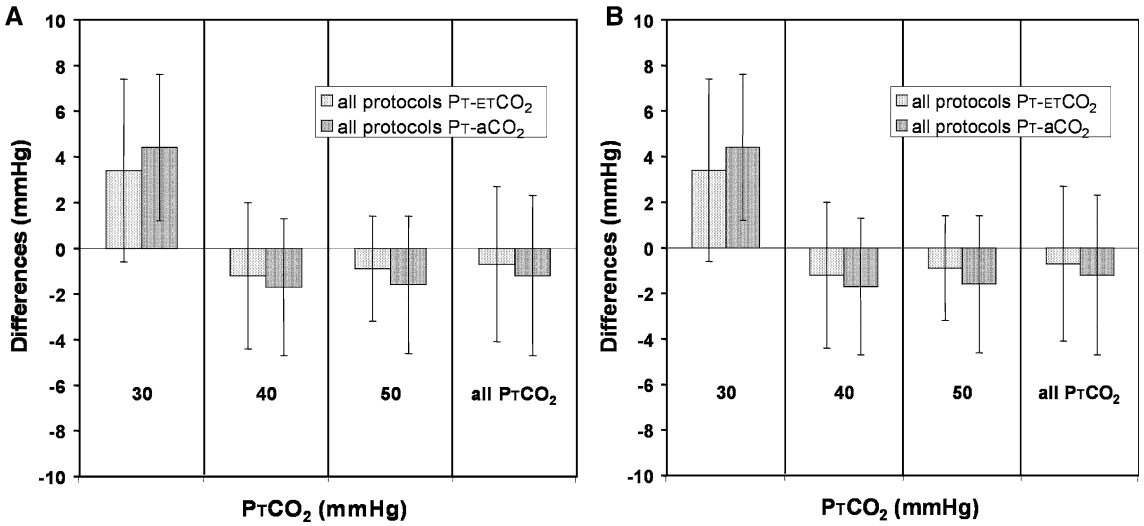

Fig. 3 **a** Mean ± SD gradients for each of the 3 protocols at each of the 3 desired PETCO2 tensions ($PTCO_2$). The gradients were between $PTCO_2$ and the measured $PETCO_2$ ($P_{T\text{-}ET}CO_2$), and between PTCO2 and the measured $PaCO_2$ ($P_{T\text{-}a}CO_2$). **b** Mean ± SD gradients for the 3 protocols combined at each of the 3 desired PETCO2 tensions ($PTCO_2$). The gradients were between $PTCO_2$ and measured $PETCO_2$ ($P_{T\text{-}ET}CO_2$) and between PTCO2 and measured $PaCO_2$ ($P_{T\text{-}a}CO_2$) values

there was sufficient power to detect a difference. $P_{ET\text{-}a}CO_2$ was greater at $PTCO_2$ of 30 mmHg ($p < 0.0001$) than at 40 or 50 mmHg ($p < 0.0001$) in each case. In every instance, $PETCO_2$ moved in the same direction as $PaCO_2$.

4 Discussion

Our study in a pediatric animal model demonstrated a $P_{ET\text{-}a}CO_2$ agreement within clinical error of measurement. This data was obtained despite abnormalities in our animals such as fetal cardiac shunts and presence of cardio-pulmonary pathology. Bland–Altman analysis of our data indicated that the agreement between $PETCO_2$ and $PaCO_2$ was 0.4 ± 2.7 mmHg (Fig. 5); an agreement not due to chance ($p < 0.0001$) [10].

The consistently small $P_{ET\text{-}a}CO_2$ in our study contrasts with those of many other studies in which $P_{ET\text{-}a}CO_2$ varies widely between subjects and in the same subjects over time. McDonald et al. [2] studied 1708 sample pairs of $PETCO_2$ and $PaCO_2$ in 129 children in an intensive care unit; $P_{ET\text{-}a}CO_2$ ranged between 0 to > −30 mmHg and only 74 % of samples changed in the same direction. Tobias and Meyer (Tobias and Meyer) [3] reported a range of $P_{ET\text{-}a}CO_2$ of 5 to −22 mmHg in 100 sample sets in 25 infants and toddlers. Nevertheless, both studies suggested that even the broad $P_{ET\text{-}a}CO_2$ in their studies of −4.7 ± 8.2 mmHg and −6.8 ± 5.1 mmHg respectively were still within a "clinically acceptable" range. Others too have found poor, or no, correlations between $PETCO_2$ and $PaCO_2$ in adults with multi-system disease [11], trauma [12], undergoing neurosurgery [5, 13], as well as in dogs with healthy lungs [14] or lungs with oleic acid-induced ARDS (Murray and others) [15].

Our findings complement those already reported in previous publications. Swenson et al. [16] were studying

Table 3 Differences between measured end-tidal PCO_2 and measured arterial PCO_2 ($P_{ET\text{-}a}CO_2$) values for each of the three protocols at each of the three target $PETCO_2$

Protocol	$PTCO_2$ (mmHg)	$P_{ET\text{-}a}CO_2$ (mmHg)	
		Mean ± SD	95 % CI
1	30	−1.2 ± 1.5	(−2.7, 0.2)
1	40	0.5 ± 2.0	(−0.2, 1.3)
1	50	0.5 ± 0.8	(−0.2, 1.1)
	Combined	0.41 ± 2.03	(−0.2, 1.0)
2	30		
2	40	0.4 ± 2.6	(−0.2, 0.9)
2	50		
	Combined	0.4 ± 2.6	(−0.2, 0.9)
3	30	−0.7 ± 3.6	(−4.0, 2.6)
3	40	0.9 ± 3.5	(−0.7, 2.5)
3	50	1.1 ± 3.9	(−2.5, 4.6)
	Combined	0.6 ± 3.6	(−0.6, 1.8)
Combined	30	−0.9 ± 2.7	(−2.5, 0.6)
Combined	40	0.5 ± 2.6	(0.1, 0.9)
Combined	50	0.7 ± 2.6	(−0.7, 2.2)
	Combined	0.4 ± 2.7	(0.0, 0.9)

$PTCO_2$ Target PCO_2, *SD* Standard deviation, *CI* Confidence interval

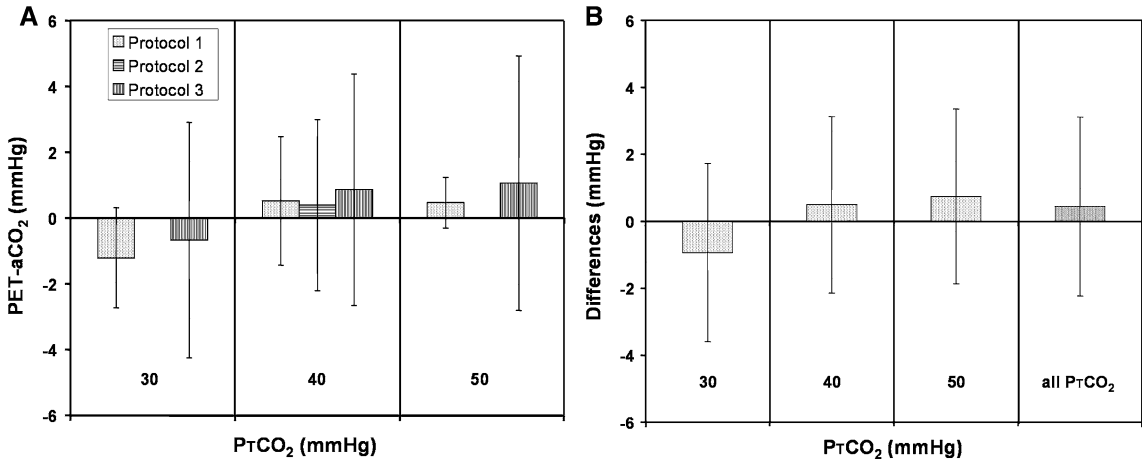

Fig. 4 **a** Mean ± SD gradient between measured $P_{ET}CO_2$ and measured $PaCO_2$ (P_{ET}-aCO_2) for each of the 3 protocols at each of the 3 desired $P_{ET}CO_2$'s tensions. **b** Mean ± SD gradient between measured $P_{ET}CO_2$ and measured $PaCO_2$ (P_{ET}-aCO_2) for all 3 protocols combined at each of the 3 desired $P_{ET}CO_2$ tensions

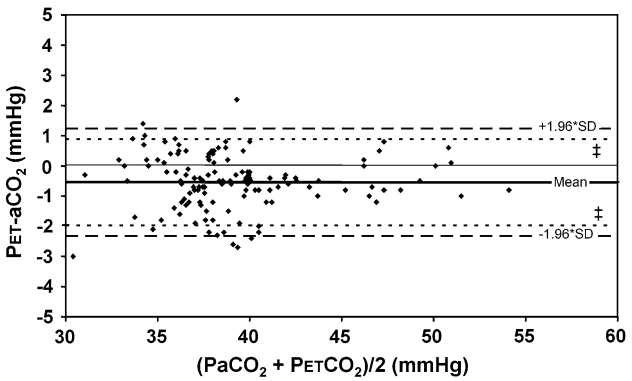

Fig. 5 The limits of agreement between $P_{ET}CO_2$ and $PaCO_2$. ‡ The *fine dotted lines* give the magnitude of the range of the P_{ET}-aCO_2 gradient due to the $PaCO_2$ measurement error alone, as calculated in a pilot study examining the P_{ET}-aCO_2 gradient in 40 kg pigs; 132 test–retest samples were analyzed with the same blood gas machine used in the current study

the effect of adding CO_2 to inspired air on reducing the alveolar to arterial PO_2 gradient (an effect first demonstrated by Ingram et al. [17] and noted that there was also a reduced gradient for CO_2, even if the CO_2 was infused at end inspiration, and distributed mainly to conducting airways [18]. No comprehensive explanation for this effect of CO_2 was offered.

Bowie et al. [19]. found that (in ventilated dogs) inhaling CO_2 in the form of rebreathing diluted exhaled gas reduced P_{ET}-aCO_2. Ito et al. [6] studied the effect of end-inspired rebreathing on P_{ET}-aCO_2 in spontaneously breathing humans. The result was a reduction in P_{ET}-aCO_2 to virtually zero. However, it was not clear that this method would remain robust in a pediatric model with positive pressure ventilation, which causes increased intra-thoracic pressure, changes in alveolar deadspace [20, 21] and affects the distribution of pulmonary blood flow [4]. Whether P_{ET}-aCO_2 would remain small over a wide range of $P_{ET}O_2$ and $P_{ET}CO_2$ tensions, both of which affect $\dot{V}/\dot{Q}$ matching [22, 23] was unknown. Indeed, some doubt has been raised whether the effect of inspired CO_2 occurs at all with large tidal volumes [16, 24]. In our animal model, we found that even with positive pressure-applied high tidal volumes, end-inspiratory rebreathing resulted in low P_{ET}-aCO_2 differences over a wide range of combinations of $P_{ET}CO_2$ and $P_{ET}O_2$.

4.1 Why end-inspiratory rebreathing reduces P_{ET}-aCO_2

Previous studies [16, 18] attributed the effect of reduction of P_{ET}-aCO_2 to the actions of CO_2 in reducing ventilation/perfusion mismatch by inducing bronchoconstriction to reduce wasted ventilation and boosting cardiac output and hypoxic pulmonary vasoconstriction to reduce the mismatch to perfusion. We explain the low P_{ET}-aCO_2 by referring to the experience with the rebreathing of previously exhaled gas to bring the $P_{ET}CO_2$ towards the $PaCO_2$ [25–27] and simulation models show this to be the case [28, 29]. It is apparent that the greater the rebreathing the smaller the fluctuations in PCO_2 and PO_2 in the alveoli within a breath, and the smaller the difference in these gases between alveoli in the lung. With the homogenization of the PCO_2 throughout the lung, heterogeneity in the distribution of pulmonary perfusion would no longer affect the $PaCO_2$ (and the end-capillary PO_2) [6]. Thus the $PaCO_2$ would approach the $PACO_2$ (as, unlike for O_2, shunted blood has minimal effect on $PaCO_2$). To address these issues, specific animal models of these lung diseases would have to be studied.

4.2 Study limitations

4.2.1 Animal model

We found that the piglets in our study were ventilated near their ventilatory capacity. Increasing peak airway pressures risked pneumothorax, and greater ventilatory frequencies risked breath stacking. We note that piglets are bred specifically for rapid muscle growth to reduce their time to market http://www.thepigsite.com/stockstds/17/growth-rate), which markedly increases their CO_2 production to 2–5 times that of a human of comparable weight, but their ventilatory capacity remains proportional to their body size. Further reducing their ventilatory reserve was the presence of extensive atelectasis. PEEP was not used in this study in order to isolate the effects of our intervention (end-inspiratory rebreathing) and to maintain a "worst case scenario". We did not induce the lung pathology nor did we carefully measure its effects on pulmonary function. As such it is not appropriate for us to apportion effect of the pathology on the results. However, it is true that the lungs in the newborn piglets were not perfectly normal and that fact suggests that our finding are likely to be more robust than had it been performed in animals perfectly healthy lungs.

4.2.2 Protocol

A limitation of our protocol was that all $P_{ET}CO_2$ and $PaCO_2$ pairs were tested only with end-inspiratory rebreathing, leaving the P_{ET}-aCO_2 gradient before rebreathing unknown. It is presumed from numerous extensive investigations published in the literature and cited above, that P_{ET}-aCO_2 gradients are frequently considerably greater than those shown in this study.

4.2.3 Quantifying the extent of rebreathing

Only the presence, rather than the extent, of end-inspiratory rebreathing could be identified in these experiments by observing a rise in the recorded PCO_2 trace at the end of the inspiratory phase. As a result, the extent of end-inspiratory rebreathing likely varied across the protocols. Despite this variation, the measured P_{ET}-aCO_2 gradients remained uniformly small. This finding implies that the threshold for effective end-inspiratory rebreathing is low. The same observation has been reported by Brogan et al. [30] in healthy dogs, with respect to unquantified, but small, volumes of CO_2 added at end inspiration. Nevertheless, there may be identifiable thresholds for rebreathing that vary with the underlying lung pathology and ventilator settings.

4.2.4 Sampling from the trachea versus from the proximal endotracheal tube

Small tidal volumes, high respiratory frequencies, and high ratios of equipment deadspace to tidal volume contribute to the sampling error with sidestream capnography. Badgewell et al. [31–33] studied this issue in considerable detail and concluded that for children less than 12 kg, accurate end-tidal measurements can only be obtained from the distal endotracheal tube. We placed the gas sampling catheter beside, rather than inside, the endotracheal tube in order to provide the least resistance for the high minute ventilations required to ventilate piglets compared to those required to ventilate humans of the same weight.

4.3 Complexity of the breathing circuit

We designed this breathing circuit to carry out a protocol that enabled the implementation of ventilatory conditions resulting in a large range of combinations of $P_{ET}CO_2$ and $P_{ET}O_2$, while maintaining end-inspiratory rebreathing. Should end-inspiratory rebreathing prove effective in predicting $PaCO_2$ from $P_{ET}CO_2$ in humans, it can be implemented with simpler modifications of standard ventilator tubing [34].

4.4 Summary and conclusion

We found that end-inspiratory rebreathing results in a small P_{ET}-aCO_2 gradient in a newborn pig model over a wide range of $P_{ET}CO_2$ and $P_{ET}O_2$. Our findings therefore demonstrate that a non-invasive surrogate test for $PaCO_2$ may be feasible but has to be verified clinically.

Acknowledgments We thank Tamara Arenovich for her assistance with the statistical analysis and Dr Steve Iscoe for his valuable contribution to the manuscript. We also thank the veterinary research team of the Animal Facility of the Hospital for Sick Children, in particular Marvin Estrada for his assistance and advice during the animal experiments. This work was supported by the Chair fund of the Neurovascular Therapeutics Program, the Department of Anesthesiology at the University Health Network, the University of Toronto; through a Merit Award to J.F; and by TRI by providing access to RespirAct™.

Conflict of Interest RespirAct™ is currently a non-commercial research tool made available for this research by TRI, a spin-off company from the University Health Network. J. A. F. and J. D. contributed to the development of the RespirAct™ and in addition to their academic positions, hold paid positions at TRI.

References

1. Berkenbosch JW, Lam J, Burd RS, Tobias JD. Noninvasive monitoring of carbon dioxide during mechanical ventilation in

older children: end-tidal versus transcutaneous techniques. Anesth Analg. 2001;92:1427–31.
2. McDonald MJ, Montgomery VL, Cerrito PB, Parrish CJ, Boland KA, Sullivan JE. Comparison of end-tidal CO2 and Paco2 in children receiving mechanical ventilation. Pediatr Crit Care Med. 2002;3:244–9.
3. Tobias JD, Meyer DJ. Noninvasive monitoring of carbon dioxide during respiratory failure in toddlers and infants: end-tidal versus transcutaneous carbon dioxide. Anesth Analg. 1997;85:55–8.
4. Wahba RW, Tessler MJ. Misleading end-tidal CO2 tensions. Can J Anaesth. 1996;43:862–6.
5. Russell GB, Graybeal JM. End-tidal carbon dioxide as an indicator of arterial carbon dioxide in neurointensive care patients. J Neurosurg Anesthesiol. 1992;4:245–9.
6. Ito S, Mardimae A, Han J, et al. Non-invasive prospective targeting of arterial P(CO2) in subjects at rest. J Physiol. 2008;586:3675–82.
7. Slessarev M, Han J, Mardimae A, et al. Prospective targeting and control of end-tidal CO2 and O2 concentrations. J Physiol. 2007;581:1207–19.
8. Robbins PA, Swanson GD, Howson MG. A prediction-correction scheme for forcing alveolar gases along certain time courses. J Appl Physiol. 1982;52:1353–7.
9. Bland JM, Altman DG. Statistical methods for assessing agreement between two methods of clinical measurement. Lancet. 1986;1:307–10.
10. Preiss D, Fisher J. A measure of confidence in Bland-Altman analysis for the interchangeability of two methods of measurement. J Clin Monit Comput. 2008;22:257–9.
11. Hoffman RA, Krieger BP, Kramer MR, et al. End-tidal carbon dioxide in critically ill patients during changes in mechanical ventilation. Am Rev Respir Dis. 1989;140:1265–8.
12. Russell GB, Graybeal JM. Reliability of the arterial to end-tidal carbon dioxide gradient in mechanically ventilated patients with multisystem trauma. J Trauma. 1994;36:317–22.
13. Russell GB, Graybeal JM. The arterial to end-tidal carbion dioxide difference in neurosurgical patients during craniotomy. Anesth Analg. 1995;81:806–10.
14. Neto FJ, Carregaro AB, Mannarino R, Cruz ML, Luna SP. Comparison of sidestream capnograph and a mainstream capnograph in mechancally ventilated dogs. J Am Vet Med Assoc. 2002;221:1582–5.
15. Murray IP, Modell JH, Gallagher TJ, Banner MJ. Titration of PEEP by the arterial minus end-tidal carbon dioxide gradient. Chest. 1984;85:100–4.
16. Swenson ER, Robertson HT, Hlastala MP. Effects of inspired carbon dioxide on ventilation-perfusion matching in normoxia, hypoxia, and hyperoxia. Am J Respir Crit Care Med. 1994;149:1563–9.
17. Ingram RH Jr, Finlay GD, Bradford FM Jr. Relationship of AaDO $_2$ to airway PCO_2 in dog lungs. J Appl Physiol. 1976;40:720–4.
18. Brogan TV, Robertson HT, Lamm WJ, Souders JE, Swenson ER. Carbon dioxide added late in inspiration reduces ventilation-perfusion heterogeneity without causing respiratory acidosis. J Appl Physiol. 2004;96:1894–8.
19. Bowie JR, Knox P, Downs JB, Smith RA. Rebreathing improves accuracy of ventilatory monitoring. J Clin Monit. 1995;11:354–7.
20. Fletcher R, Jonson B. Deadspace and the single breath test for carbon dioxide during anaesthesia and artificial ventilation. Effects of tidal volume and frequency of respiration. Br J Anaesth. 1984;56:109–19.
21. Tusman G, Suarez-Sipmann F, Bohm SH, et al. Monitoring dead space during recruitment and PEEP titration in an experimental model. Intensive Care Med. 2006;32:1863–71.
22. Larson C, Severinghaus JW. Postural variations in dead space and CO2 gradients breathing air and O2. J Appl Physiol. 1962;17:417–20.
23. Anderson KJ, Harten JM, Booth MG, Kinsella J. The cardiovascular effects of inspired oxygen fraction in anaesthetized patients. Eur J Anaesthesiol. 2005;22:420–5.
24. Bradford JM Jr, Ingram RH Jr, Davis J, Finlay GD. Relationship of alveolar CO_2 and O_2 pressures to AaDo2 in normal subjects. J Appl Physiol. 1974;37:139–44.
25. Read DJ. A clinical method for assessing the ventilatory response to carbon dioxide. Australas Ann Med. 1967;16:20–32.
26. Casey K, Duffin J, McAvoy GV. The effect of exercise on the central-chemoreceptor threshold in man. J Physiol. 1987;383:9–18.
27. Mohan RM, Amara CE, Cunningham DA, Duffin J. Measuring central-chemoreflex sensitivity in man: rebreathing and steady-state methods compared. Respir Physiol. 1999;115:23–33.
28. Read DJ, Leigh J. Blood-brain tissue Pco2 relationships and ventilation during breathing. J Appl Physiol. 1967;23:53–70.
29. Duffin J. Measuring the respiratory chemoreflexes in humans. Respir Physiol Neurobiol. 2011;177:71–9.
30. Brogan TV, Robertson HT, Lamm WJ, Souders JE, Swenson ER. Carbon dioxide added late in inspiration reduces ventilation-perfusion heterogeneity without causing respiratory acidosis. J Appl Physiol. 2004;96:1894–8.
31. Hillier SC, Badgwell JM, McLeod ME, Creighton RE, Lerman J. Accuracy of end-tidal PCO2 measurements using a sidestream capnometer in infants and children ventilated with the Sechrist infant ventilator. Can J Anaesth. 1990;37:318–21.
32. Badgwell JM, Heavner JE, May WS, Goldthorn JF, Lerman J. End-tidal PCO2 monitoring in infants and children ventilated with either a partial rebreathing or a non-rebreathing circuit. Anesthesiology. 1987;66:405–10.
33. Badgwell JM, McLeod ME, Lerman J, Creighton RE. End-tidal PCO2 measurements sampled at the distal and proximal ends of the endotracheal tube in infants and children. Anesth Analg. 1987;66:959–64.
34. Fierstra J, Machina M, Battisti-Charbonney A, Duffin J, Fisher JA, Minkovich L. End-inspiratory rebreathing reduces the end-tidal to arterial PCO2 gradient in mechanically ventilated pigs. Intensive Care Med. 2011;37:1543–50.